IEEE Access
The journal for rapid open access publishing

Received May 12, 2015, accepted June 7, 2015, date of publication June 16, 2015, date of current version June 26, 2015.

Digital Object Identifier 10.1109/ACCESS.2015.2445976

Semi-Persistent RRC Protocol for Machine-Type Communication Devices in LTE Networks

YINAN QI, (Member, IEEE), ATTA UL QUDDUS, (Member, IEEE), MUHAMMAD ALI IMRAN, (Senior Member, IEEE), AND RAHIM TAFAZOLLI, (Senior Member, IEEE)

Institute for Communication Systems, University of Surrey, Guildford GU2 7XH, U.K.

Corresponding author: Y. Qi (yinan.qi@surrey.ac.uk)

This work was supported in part by the University of Surrey, Guildford, U.K., through the 5G Innovation Centre Programme, and in part by Sony Europe Ltd., Surrey, U.K.

ABSTRACT In this paper, we investigate the design of a radio resource control (RRC) protocol in the framework of long-term evolution (LTE) of the 3rd Generation Partnership Project regarding provision of low cost/complexity and low energy consumption machine-type communication (MTC), which is an enabling technology for the emerging paradigm of the Internet of Things. Due to the nature and envisaged battery-operated long-life operation of MTC devices without human intervention, energy efficiency becomes extremely important. This paper elaborates the state-of-the-art approaches toward addressing the challenge in relation to the low energy consumption operation of MTC devices, and proposes a novel RRC protocol design, namely, semi-persistent RRC state transition (SPRST), where the RRC state transition is no longer triggered by incoming traffic but depends on pre-determined parameters based on the traffic pattern obtained by exploiting the network memory. The proposed RRC protocol can easily co-exist with the legacy RRC protocol in the LTE. The design criterion of SPRST is derived and the signalling procedure is investigated accordingly. Based upon the simulation results, it is shown that the SPRST significantly reduces both the energy consumption and the signalling overhead while at the same time guarantees the quality of service requirements.

INDEX TERMS 3GPP, LTE, radio resource control (RRC), machine type communication (MTC), discontinuous reception (DRX).

I. INTRODUCTION

With the revolution of innovative silicon technologies, the end-user devices are becoming ''bigger'' and ''smaller'' at the same time in the sense that they are more sophisticated and capable of conducting a variety of functionalities while at the same time they shrink in size that paves the way of the development of more sleek and lightweight devices for machine type communication (MTC), also known as machine to machine (M2M) communication. M2M communication refers to exchange of information (whether wireless or wired) to and from uniquely identifiable objects and their virtual representations in an Internet-like structure without human involvement. This creates a new ecosystem-system that gives rise to a plethora of interesting applications and new business opportunities, and hence it is considered to be a potential enabling technology for the emerging paradigm of the new generation of application driven networks [1], [2].

MTC has its own peculiar constraints, such as access limitations and lack of human intervention, which motivates energy efficient operation with varying degrees of importance. Some MTC devices can be connected to a stable power supply source and hence reduced energy consumption is only desired in order to reduce energy bills. However, the saving in energy bills can be negligible given the low data rate and infrequent communication requirements for MTC. In many other scenarios, such as remote industrial areas, extra low energy consumption is required for MTC devices due to the constraints of limited resources of energy in the form of a battery which could be infeasible to be replaced on a frequent basis. An example of such an MTC device, which has low mobility requirements, is a smart meter.

For high mobility MTC devices low energy consumption is also required to avoid battery replacement, e.g., tracking devices installed on animals in the wild world for research purposes, require extra low energy consumption as well

because it is very difficult, if not impossible, to replace or recharge the batteries. For other application scenarios such as cargo, body sensors, medical implants, prisoners and children tracking, low energy consumption is also critical since a copious power supply source is missing and a battery is not easily accessible [3].

Considering the reasons given above, low energy consumption for MTC devices is identified as one of the key issues in the 3rd Generation Partnership Project (3GPP) that is one of the main standardization bodies, and several EU research projects, such as C2POWER and EXALTED [4], [5]. Some research ideas in this area are incorporated in 3GPP release 11 [6] and this topic is one of the main focuses in 3GPP release 13 [7]. It is required by 3GPP to improve the system design for providing mechanisms to lower the energy consumption of MTC Devices [5]. In order to achieve this reduction in energy consumption, we need to understand the areas where there are better opportunities to save energy. In this regards, the overall MTC device energy consumption is broken down in a 3GPP study [8], [9] to illustrate the percentage consumption of each sub-system and some important contexts are mentioned for user equipment (UE) power optimization in [9] and [10] as: (1) extended discontinuous reception (DRX) to prevent battery drain, (2) introduction of a new power saving state, where a UE may adopt when there are longer periods of inactivity, and (3) introduction of a new low complexity UE category type that supports reduced transmit power. The energy consumption needs to be reduced both in idle and standby modes as well as the actual operation of the transceiver. Since several types of MTC devices spend the majority of their time in idle mode, this context of energy efficient operation becomes an area of paramount importance.

Various solutions for extra low energy consumption MTC devices have been proposed in the literature from different perspectives, see [11]–[14] where the network operations including routing and scheduling is optimized to minimize the impact on device's battery usage. As mentioned previously, DRX is proposed to save energy in LTE and LTE-A networks [15]–[21]. The idea of DRX is that a UE is only activated for a short period of time to check the incoming data and gets into sleep-mode for a long period of time if no data is coming. The interval between the beginnings of two UE activation periods is defined as DRX cycle. The power saving potentials of DRX are analysed in [18] and [19] and it is proposed to use a mixture of short and long cycles to further improve the effectiveness of DRX mechanism. Clearly, DRX mechanism will cause latency issue because the packets that arrive during sleep-mode have to wait until the UE is activated. The trade-off between energy saving and latency is studied in [20] and [21], where effective DRX configurations are proposed to increase the energy saving without significant increase in latency of active traffic. However, it is pointed out in [22]–[24] that even with DRX, the energy consumption of LTE devices is still significantly larger than 3G and WiFi devices, especially for small data packet transmission that happens to be one of the most typical and important cases in MTC Communication. It implies that the current state of the art mobile communication systems, e.g., LTE and LTE-A, are not designed to support the new paradigm of MTC and therefore rethinking the way of designing the cellular networks is becoming more and more important. It is towards this objective this paper intends to make a contribution.

One of the potential areas to improve energy efficiency is the design of Radio Resource Control (RRC) protocol, specifically for MTC devices. The normal RRC mechanism in LTE is investigated in [25] and [26], where RRC_Connected and RRC_Idle states are defined for UEs being in active-mode and sleep-mode, respectively. The statistics of RRC state transition is studied in [27] in order to approximate the distribution of mobile users in RRC_Connected state. Further enhancement of RRC mechanism is presented in [28] to reduce signalling overhead when establishing RRC connections. However, considering the unique characteristics of MTC devices, following issues can be identified in the current LTE RRC procedure:

1) The long inter-arrival time of MTC traffic is not taken into consideration, which is typically a couple of tens of seconds [8]. During this long inter-arrival period, a UE wakes up periodically to check the paging message, which drains the UE battery;
2) Additionally, due to the long inter-arrival time, once the RRC connection is established, there is normally only one MTC packet to be transmitted/received in most of the cases and a few hundred bits signalling overhead is then added on top of each MTC packet [25];
3) The extremely low mobility, or zero mobility scenario, for certain MTC devices, e.g., smart meters, is not considered.

In this paper, we propose a novel Radio Resource Control (RRC) procedure suitable for MTC communication to reduce both the energy consumption of MTC devices and the signalling overhead for LTE networks. The main contributions can be summarized as follows:

1) Based on the MTC traffic parameters obtained by exploiting the network memory, a novel RRC protocol is designed by taking into account the unique characteristics of MTC devices, e.g., small packet transmission, low mobility, and high latency tolerance;
2) The delay and signalling overhead of the proposed RRC protocol are analysed and probability density function (pdf) and cumulative density function (CDF) of delay are derived. Furthermore, the design criterions of the proposed protocol subject to certain QoS requirements are provided;
3) Comprehensive energy consumption analysis and comparison based on an empirically derived power model [22] of a commercial LTE network is conducted for the current and proposed RRC protocols;
4) Additionally, system level simulations are carried out to evaluate the efficiency of the proposed RRC protocol

from the perspectives of delay, signalling overhead and energy consumption for typical MTC traffic patterns in the framework of 3GPP LTE, where MTC devices and normal LTE devices co-exist.

The rest of the paper is organized as follows. The current RRC procedure and DRX operation in LTE networks are briefly introduced in the next section. In section III, the novel RRC protocol design is presented and the design criterions and energy consumption analysis are given. In section IV, system level simulation results are presented with some discussions and thereafter section V concludes the paper.

II. RRC PROTOCOL AND DRX OPERATION IN LTE NETWORKS

RRC protocol layer exists in both the UE and eNodeB (eNB) and provides main services and functions such as paging, establishing and releasing of an RRC connection, etc. In this section, we will very briefly introduce the RRC state transition and the DRX procedure in the current LTE networks.

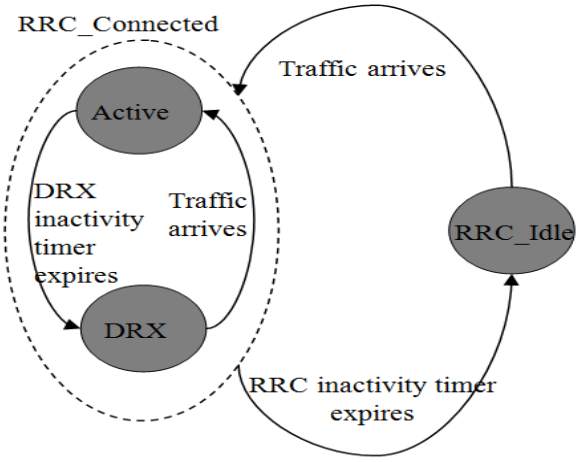

FIGURE 1. RRC state transition in LTE.

A. RRC PROCEDURE IN LTE NETWORKS

As shown in Fig. 1, there are two states for LTE UEs: RRC_Idle and RRC_Connected [25]. In RRC_Idle state, a UE has already registered with the network but is not connected and thus there is no radio link established between the network and itself. The UE needs to monitor a paging channel to detect incoming traffic, acquires system information and performs neighbouring cell measurement and cell reselection. Once downlink (DL)/uplink (UL) traffic activity happens, the UE is moved to RRC_Connected, where it has an Evolved-Universal. Terrestrial Radio Access Network (E-UTRAN) RRC connection and the network can transmit/receive data to/from the UE. After the eNB has cleared its transmission (Tx) buffer and does not detect any uplink data from the UE, a UE inactivity timer is activated. Once the UE inactivity timer expires, a RRC connection release message is sent from the network and the UE goes back to RRC_Idle state.

B. DRX OPERATION IN LTE NETWORKS

DRX can be configured for both RRC_Idle and RRC_Connected states. In RRC_Idle state, the UE only monitors Physical Downlink Control Channel (PDCCH) at pre-determined occasions and during the rest of time, it goes to sleep to save energy. In RRC_Connected state, in order to reduce latency in physical layer transmission a number of timers enforcing additional active time for the UE reception (Rx) circuitry are used. The details of DRX operation and the meaning of these timers are explained in Appendix A.

The current RRC protocol and DRX operation are designed targeting the UEs with high traffic demand, where it is assumed that once a new traffic packet arrives and a RRC connection is established, more following traffic packets are expected to arrive. Thus it would be more efficient to wait for the following packets in the RRC_Connected state rather than switching back to RRC_Idle state immediately after the transmission of the current packet to avoid frequent RRC state transitions. However, considering the unique properties of MTC devices with very low traffic volume, infrequent and intermittent data bursts and low mobility in many cases, no follow up packets is expected thus waiting for the next packet in RRC_Connected state will cause unnecessary energy consumption. This incompatibility between RRC and DRX protocol design and MTC device requirements is a key problem whose solution has the potential for improving the energy efficiency of the MTC devices.

III. PROPOSED SEMI-PERSISTENT RRC STATE TRANSITION PROTOCOL

A Semi-Persistent RRC State Transition (SPRST) scheme is proposed in this section for saving the energy of MTC devices. This scheme makes use of the network memory and can be divided into a measurement stage and a SPRST stage as shown in Fig. 2 and the defined new timers and related parameters are summarized in Table 1.

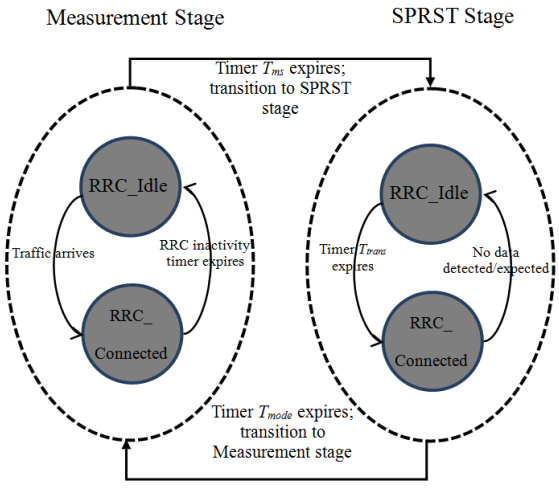

FIGURE 2. Stage transition of the proposed scheme.

TABLE 1. New timers and related parameters.

Parameter	Description
T_{ms}	The duration of measurement stage
T_{mode}	The duration of SPRST stage
T_{trans}	RRC transition cycle
T_{int}	Mean inter-arrival time of packets

A. RRC STATE TRANSITION MECHANISM

The objective of the measurement stage is to obtain key statistical characteristics of the MTC traffic. Assuming Poisson process for MTC traffic [8], the key traffic parameter to be measured is the mean packet inter-arrival time T_{int}. It should be noted that some studies have revealed that there exist some traffic types that do not satisfy the conditions of Poisson process. In such cases, the proposed RRC protocol design should be modified to improve energy efficiency and at the same time satisfy the QoS requirements. However, this is out of the scope of this work and will be of great interest to be investigated in the future.

In 3GPP at the MTC Work Item in Radio Access Network Working Group 2 (RAN WG2) [29], it was discussed that the Core Network (CN) could provide statistics on packet inter-arrival times for all the radio bearers of a UE based upon global observations. An alternative approach would be to determine the inter-arrival times at the eNBs based on local measurements. In either case, measurements need to be made and we assume that the duration of measurement stage is T_{ms} which could be different for each UE. In this stage, normal RRC transition and DRX procedures are carried out.

Once the measurement stage is complete, i.e., timer T_{ms} expires, and T_{int} is obtained, the eNB should notify the UE to enter the SPRST stage as depicted in Fig. 2. For this purpose, a single bit information defined as SPRST indicator can be sent from the eNB to the UE. The duration of the SPRST stage is determined by a timer T_{mode} at the eNB. Once T_{mode} expires, the eNB sends the SPRST indicator bit to notify the UE to move back to the measurement stage with normal RRC operation.

The flow chart of the operations for the eNB and UE is provided in Fig. 3. In the SPRST stage, unlike the current RRC procedure where the RRC transition from RRC_Idle to RRC_Connected is triggered by the incoming traffic, a new timer T_{trans} is defined to control the state transition. This timer is determined depending on the traffic pattern characterized by T_{ini} and other Quality of Service (QoS) requirements which are discussed later in section III.B and should be sent by the eNB to the UE during the RRC establishment procedure. If a packet arrives at the eNB before T_{trans} expires, this packet is buffered at the eNB. At the UE side, the UE keeps silent without being activated to check the paging messages periodically. Once the timer T_{trans} expires, the UE starts the Random Access Procedure (RAP) by sending the random access (RA) preamble to the eNB followed by the RRC establishment procedure, and T_{trans} can

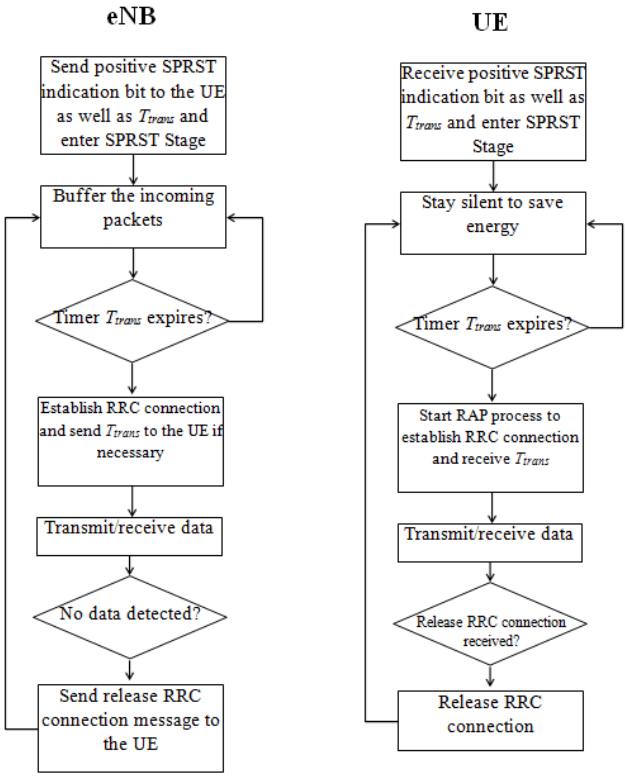

FIGURE 3. Flow chart.

be reset immediately if necessary. In other words, every time T_{trans} expires, the network automatically performs RRC transition from RRC_Idle state to RRC_Connected state, i.e., the RRC transition happens periodically depending solely on T_{trans} but not on the incoming traffic. Thus there is no need for the UE to periodically check paging messages in RRC_Idle state and the consumed energy can be saved. This scheme is named as semi-persistent scheme because the value of the timer T_{trans} is constant over a period of time but can be changed from time to time. An extreme case is persistent RRC state transition where the value of T_{trans} is constant during the whole operation of SPRST stage. Different from DRX, which operates within each RRC state, the proposed strategy works on RRC layer directly and it can easily co-exists with other LTE UEs applying normal RRC protocol.

In the existing LTE systems, as mentioned before, a RRC inactivity timer is required to command the UE to move back to RRC_Idle state. In the SPRST protocol, this timer is no longer needed. The eNB sends the RRC release message once the buffer is cleared and no UL data is detected or expected. Without the UE inactivity timer, the UE is expected to stay in DRX mode of RRC_Connected state for a very short time before moving back to RRC_Idle state. This will provide further energy saving potentials as will be shown in the simulation section.

B. DESIGN CRITERIONS OF RRC TRANSITION CYCLE T_{trans}

The design of T_{trans} is subject to three pre-defined service requirements: delay tolerance, false transmission

probability and average signalling overhead ratio. They are further explained below.

1) DELAY TOLERANCE

In the SPRST stage, it is expected that the transmission endures certain level of delay because as long as the system is in RRC_Idle state, the arrived packets are buffered at the eNB and wait for the RRC state transition. Clearly, the delay, denoted as T_d, is a random variable and the longer the T_{trans}, the larger the delay is envisaged. There are three different ways to demonstrate the delay caused by the SPRST protocol: (1) maximal delay T_{max}, (2) average delay T_{ave}, and (3) probability delay T_P which indicates that with a given target probability P, we have Prob $\{T_d \leq T_P\} = P$. The maximal delay T_{max} is equal to $T_{trans} - T_{fal}$, where T_{fal} is the duration of the UE staying in RRC_Connected state but has nothing to transmit/receive. If $T_{fal} \ll T_{trans}$, T_{max} can be approximated by T_{trans}.

In order to obtain T_{ave} and T_P, we need to derive the probability density function (pdf) of the random variable T_d.

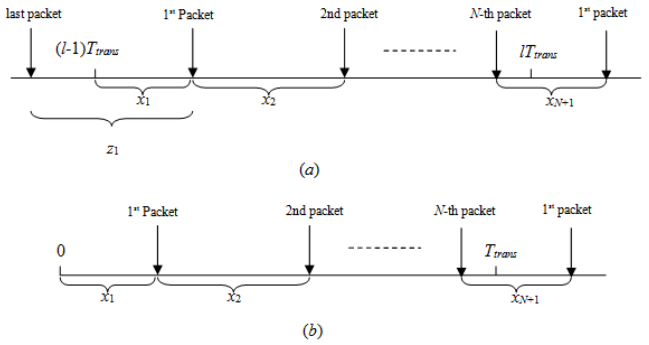

FIGURE 4. MTC packets arrival process. (a) Poisson process. (b) Simplified Poisson process.

Assuming Poisson process for MTC traffic with mean arrival rate $\lambda = 1/T_{ini}$ as shown in Fig. 4 (a), we consider the general case where N packets are assumed to arrive between time $(l-1)T_{trans}$ and lT_{trans}. The n-th packet arrives at time

$$s_n = (l-1)\,T_{trans} + \sum_{i=1}^{n} x_i, \tag{1}$$

where x_i is the inter-arrival time between packet (i-1) and i except x_1. Since all the packets arrived during time [(l-1)T_{trans}, lT_{trans}) are buffered at the eNB and sent until time lT_{trans}, the delay of the n-th packet is given as

$$d_n = lT_{trans} - (l-1)\,T_{trans} - \sum_{i=1}^{n} x_i = T_{trans} - \sum_{i=1}^{n} x_i. \tag{2}$$

For the first packet, the inter-arrival time between itself and the previous packet is z_1. Clearly, z_1 and x_2 to x_N follow the exponential distribution and are independent from each other. If $l = 1$, $z_1 = x_1$; otherwise $z_1 \geq x_1$. However, according to [30], x_1 also follows the exponential distribution and is independent from x_2 to x_N. This means that d_n has no relevance to l so that we can consider a simplified case as shown in Fig. 4 (b) and we have

$$s_n = \sum_{i=1}^{n} x_i, \tag{3}$$

where s_n follows the Erlang distribution [30].

If $N = 1$, i.e., there is only one packet arrived during time [0, T_{trans}). The joint density for X_1 and S_2 is

$$f_{X_1S_2}(x_1, s_2) = f_{X_1}(x_1) f_{X_2}(s_2 - x_1). \tag{4}$$

The marginal density of S_2 can be obtained by integrating X_1 out from the joint density, which takes the form:

$$\begin{aligned} f_{X_1S_2}(x_1, s_2) &= \lambda^2 \exp(-\lambda x_1) \exp(-\lambda(s_2 - x_1)) \\ &= \lambda^2 \exp(-\lambda s_2), \quad \text{for} \quad 0 \leq x_1 \leq s_2. \end{aligned} \tag{5}$$

Obviously, the jointly density does not contain x_1. Thus, for a fixed s_2, the conditional density of X_1 given $S_2 = s_2$ is uniform over $0 \leq x_1 \leq s_2$. Considering $N = 1$, it implies that $T_{trans} \leq s_2$ so that the conditional density of X_1 is also uniform over $0 \leq x_1 \leq T_{trans}$. It is easy to see that the delay d_n also follows the uniform distribution over [0, T_{trans}).

For the more general cases, the same behaviour is observed here as

$$\begin{aligned} f_{S_1S_{N+1}}(s_1, \ldots, s_N, s_{N+1}) &= \lambda^2 \exp(-\lambda s_{N+1}), \\ &\text{for } 0 \leq s_1 \leq \cdots s_N \leq s_{N+1}. \end{aligned} \tag{6}$$

The joint density does not contain any arrival time other than s_n, except for the ordering constraint $0 \leq s_1 \leq \ldots \leq s_{N+1}$, and thus this joint density is constant over all choices of arrival times satisfying the ordering constraint. If any s_n is uniformly distributed, the delay d_n is also uniformly distributed and the pdf and CDF functions are, respectively,

$$p(d_n) = \frac{1}{T_{trans}}, \quad F(d_n) = \frac{1}{T_{trans}} d_n, \quad \text{for} \quad 0 \leq d_n \leq T_{trans}. \tag{7}$$

This equation reveals a very important conclusion that the distribution of the delay is solely determined by T_{trans} and bears no relevance to the inter-arrival time. Then we have

$$T_{ave} = T_{trans}/2, \quad T_P = PT_{trans}. \tag{8}$$

Even though the machine type traffic is usually delay tolerant, it does not mean that the MTC devices can stand infinite delay. We thereby identify three constraints on the delay in this work. In order to satisfy all the constraints identified in (8), T_{trans} is given as

$$T_{trans} \leq \min\{T_{\max}, 2T_{ave}, T_P/P\}. \tag{9}$$

2) FALSE TRANSITION PROBABILITY

$P_{fal} - P_{fal}$ is defined as the probability that no data packet arrives during T_{trans} so that although the RRC transition is conducted, no data is transmitted after the RRC connection is established. Thus the energy consumed by the signalling exchange is wasted. Generally speaking, the shorter the T_{trans},

the smaller the false possibility is. The false transition probability P_{fal} can be easily obtained based on the distribution of the Poisson process as

$$P_{fal} = \exp(-\lambda T_{trans}). \quad (10)$$

Given a target P_{fal}, we should have

$$T_{trans} \geq -T_{int} \ln P_{fal}. \quad (11)$$

3) SIGNALLING OVERHEAD RATIO

Another factor that needs to be considered is the signalling overhead ratio, i.e., signalling overhead per packet. Since the MTC traffic is generally intermittent bursty data packets, the relative amount of signalling over user plane data could be very large because RRC connection establishment and release require a few hundred bits at a time for very small amount of data to be transmitted [25]. In this regard, it is more efficient that multiple packets are buffered at the eNB and transmitted to the MTC UE in one occasion of RRC connection establishment and release. The SPRST protocol inherently fits to implement this idea. Assuming that at least K packets are transmitted with one RRC transition (signalling overhead ratio $1/K$) with a probability of P_K, it can be expressed as

$$P_K = 1 - \sum_{k=0}^{K-1} \frac{\exp(-\lambda T_{trans})(\lambda T_{trans})^k}{k!} = f(T_{trans}), \quad (12)$$

where $f(.)$ is defined as a function of T_{trans} as illustrated in (12). Then the constraint is

$$T_{trans} \geq f^{-1}(P_k). \quad (13)$$

Combining the three constraints, we have

$$\max\left\{f^{-1}(P_k), -T_{int} \ln P_{fal}\right\} \leq T_{trans} \leq \min\{T_{\max}, 2T_{ave}, T_P/P\}. \quad (14)$$

There is generally a requirement that the eNB should know whether the particular MTC UE that is being paged is under its cell. Considering the fact that some MTC devices are with extremely low mobility or even static, it is unlikely that the UE will be associated with a different eNB during the whole process and thus the aforementioned constraints can be satisfied. It should be noted that estimation of T_{int} during the measurement stage might not be accurate and with this estimation error the design might not be able to meet the QoS requirements, such as latency. However, we assume perfect estimation in this paper and leave the analysis of estimation error for future work.

C. ENERGY CONSUMPTION ANALYSIS

The energy consumption analysis is based on the empirical power models derived from a commercial LTE network [22] and the parameters and power consumption are summarized in Table 2. Here we only focus on DL data and since the impact of UL ACK/NACK is minor and their energy consumption is ignored.

TABLE 2. Parameters and power model [22].

Parameter	Name	Description	Power
T_i	*drx-InactivityTimer*	UE can continuously receive data for T_i without DRX	P_{data} : consumed power when UE receives data. P_{Ton}: consumed power when data reception is complete and the UE checks PDCCH of each subframe.
T_{is}	*shortDRX-CycleTimer*	UE stays in short DRX mode for T_{is}	N/A
T_{on}	*onDurationTimer (RRC_Connected)*	UE is active for T_{on} to check PDCCH	P_{Ton}: consumed power when the UE is active to check PDCCH in RRC_Connected.
T_{oni}	*onDurationTimer (RRC_Idle)*	UE is active for T_{on} to check paging message	P_{Toni}: consumed power when the UE is active to check paging in RRC_Idle.
T_{ps}	*Short DRX Cycle*	Cycle period of short DRX	P_{Tps}: base power when UE is in sleep during shor DRX cycle.
T_{pl}	*Long DRX Cycle*	Cycle period of long DRX	P_{Tpl}: base power when UE is in sleep in long DRX cycle.
T_{pi}	*DRX Cycle (RRC_Idle)*	Cycle period in RRC_Idle	P_{Tpi}: base power when UE is in sleep in RRC_Idle DRX cycle.
T_{prom}	*Promotiom time*	UE spends T_{prom} to transit from RRC_Idle to RRC_Connected	P_{prom}: power consumed during promotion
T_{tail}	*RRC-InactivityTimer*	UE stays in long DRX cycle mode for T_{tail} before transiting to RRC_Idle	N/A

When the UE is in RRC_Idle, the energy consumption in one DRX cycle is

$$E_{Idle} = (T_{pi} - T_{oni}) P_{Tpi} + T_{oni} P_{Toni}. \quad (15)$$

The procedure that the UE transits from RRC_Idle to RRC_Connected is called promotion [22] and the promotion energy consumption is

$$E_{prom} = T_{prom} P_{prom}. \quad (16)$$

In RRC_Connected state data reception starts once PDCCH indicates a new transmission from the eNB. In the meantime, DRX inactivity timer starts. The energy consumption is

$$E_{data} = T_{data} P_{data} + (T_i - T_{data}) P_{Ton}, \quad (17)$$

where T_{data} is the data transmission time depending on the size of the data block and allocated resources and P_{data} is the power given by a linear function of throughput t_d

$$P_{data} = \alpha_d t_d + \beta. \quad (18)$$

In the current LTE RRC protocol, once the DRX inactivity timer expires, the UE moves to short DRX cycle and short

DRX cycle timer starts. The energy consumption is

$$E_s = \frac{T_{is}}{T_{ps}} \left(\left(T_{ps} - T_{on} \right) P_{Tps} + T_{on} P_{Ton} \right). \quad (19)$$

After the short DRX cycle timer expires, the UE moves to long DRX cycle and the RRC inactivity timer T_{tail} starts. The energy consumption is

$$E_{tail} = \frac{T_{tail}}{T_{pl}} \left(\left(T_{pl} - T_{on} \right) P_{Tpl} + T_{on} P_{Ton} \right). \quad (20)$$

Therefore, the overall energy consumption for one RRC establishment/release is given as

$$E_{RRC} = N_{Idle} E_{Idle} + E_{prom} + E_{data} + E_s + E_{tail}, \quad (21)$$

where N_{Idle} is the number of DRX cycle in RRC_Idle before transition to RRC_Connected.

In the SPRST protocol, paging is not needed in RRC_Idle as mentioned before and then the consumed energy is given as $E_{Idle\_SPRST} = T_{pi} P_{Tpi}$. The promotion and data transmission energy is the same as the current RRC protocol. However, the RRC inactivity timer is no longer needed as mentioned previously. Actually, the short DRX cycle timer is not needed either thus the overall energy consumption is merely

$$E_{SPRST} = N_{Idle} E_{Idle\_SPRST} + E_{prom} + E_{data}. \quad (22)$$

IV. SIMULATION RESULTS

In this section, we assume that the MTC traffic follows Poisson process and demonstrate the improvement of the proposed new RRC protocol.

We first verify the distribution of the delay given T_{trans} with standalone simulation. It should be noted that the actual delay for a packet not only includes the time when it stays in the buffer, denoted as T_{buffer}, but also the promotion time T_{prom} during which the RRC state transition happens, the time when the packet is being transmitted in RRC_Connected state, denoted as T_{rc}, and propagation delay T_{pg} as

$$T_{latency} = T_{buffer} + T_{prom} + T_{rc} + T_{pg}. \quad (23)$$

The distribution derived in the previous section only takes T_{buffer} in to account but as long as the mean inter-arrival time is long enough so that $T_{buffer} \gg T_{prom} + T_{rc} + T_{pg}$, $T_{latency}$ can be approximated as T_{buffer}. Fig. 5 depicts the Cumulative Distribution Function (CDF) of the buffering delay T_{buffer} with mean inter-arrival time $T_{trans} = 1$. Clearly, the Monte-Carlo simulation results coincide with ideal uniform distribution, which confirms the conclusion in (7).

System level performance evaluation is then performed based on the parameters in Table 3. It is proposed in 3GPP that MTC devices should operate on reduced frequency bandwidth to co-exist with other normal LTE devices, such as smart phones and laptops [31]. In this regard, we assume that the MTC devices only occupy the central 6 Physical Resource Blocks (PRBs) and the rest of the PRBs are used by normal LTE UEs, which is in line with assumptions adopted in 3GPP work item [8].

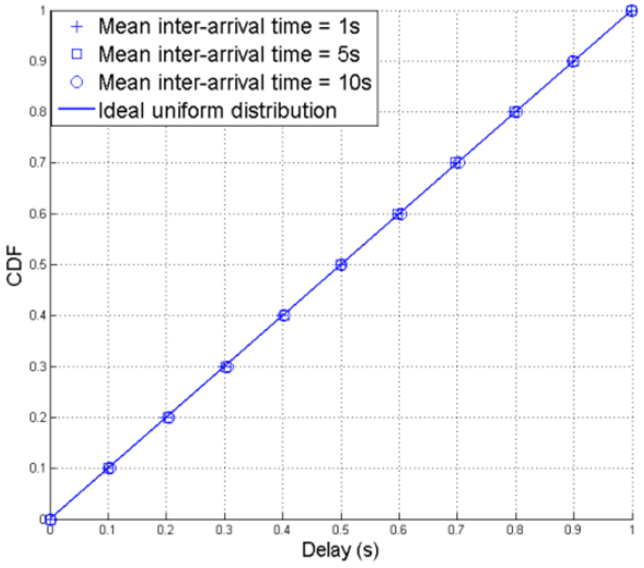

FIGURE 5. CDF of delay.

As stated earlier, T_{trans} should be designed subject to certain constraints. Considering a smart meter application scenario with high latency tolerance, here we make the following assumptions: 1) Maximal delay = 250s, 2) Average delay $\leq$ 100s, 3) 99 percent of delay should be smaller than 200s, 4) False transition probability $P_{fal} \leq 0.05$, and 5) Once the RRC connection is established, the probability of transmitting at least 2 packets is more than 90%, i.e., $P_K \geq 0.9$ ($K = 2$). Based on (8)-(14), we have

$$\max \left\{ f^{-1}(0.9) = 160, -T_{int} \ln 0.05 = 89.87 \right\} \leq T_{trans}$$

and

$$T_{trans} \leq \min \{ T_{\max} = 250, 2T_{ave} = 200, T_P/P = 202.2 \}. \quad (24)$$

Thus T_{trans} should be chosen in the range of [160,200] and we can define $T_{trans} = (T_{min} + T_{max})/2 = 180$.

When a packet arrives during RRC_Idle state, it will be saved in the buffer of the eNB. Fig. 6 plots the CDF of the number of buffered packets in the eNB with different mean inter-arrival time. We notice that for a given T_{trans}, a shorter mean inter-arrival time will increase the probability of a packet being buffered and thus will cause a larger queue size at the eNB. The maximal queue size is increased from 19 to 21 packets for $T_{trans} = 20$ s and 30 s, respectively. Generally speaking, because the packet size of MTC traffic is small and the inter-arrival time is large, it is unlikely for the proposed SPRST protocol to cause any buffer overflow problem. It should be noted that all the packets in the buffer can be sent with only one signalling overhead. The average queue size is 8 packets so that the average signalling overhead ratio is reduced to approximately 1/8.

Fig. 7 depicts the CDF of latency $T_{latency}$ with different number of MTC UEs per sector and packet sizes.

TABLE 3. Simulation parameters.

Parameter	Value
Duplex method	Frequency Division Duplexing (FDD)
Carrier freq/Band width	2GHz, 10MHz
Physical Resource Blocks (PRB)	50
MTC PRB	6
Cellular layout	Hexagonal grid, 7 macro eNB cell sites, 3 cells per site, wrap-around
MTC UE location distribution	Uniform
MTC UE per sector	50 and 500
MTC UE mobility model	Static
Tx power	46 dBm
Noise figure	-171 dBm/Hz
Scheduling	Round Robin
Downlink receiver type	2×1 MISO with 2 Tx antennas and 1 Rx antenna
Pathloss model	Macro – UE: PL = 128.1+37.6log10(R), [32] R in km
Antenna Gain	For eNBs, $G_{eNB}(\Theta) = G_{\max} - \min\left\{12\left(\frac{\Theta}{\Theta_{3dB}}\right)^2, G_{f2b}\right\}$, $-180° \le \Theta \le 180°$ where G_{max}=14dBi, Θ is the angle between the eNB-UE line of sight and the sector boresight, Θ_{3dB} is the angle spread for 3dB attenuation, and G_{f2b} is the antenna front to back ratio. [32] For MTC UEs, omnidirectional antenna is assumed with 0dB antenna gain.
Shadow	Macro: 8 dB, site-to-site correlation = 0.5
Channel model	No fast fading
MTC traffic model	Mean inter-arrival time = 30s, packet size = 256 bits, 1000bits [8]

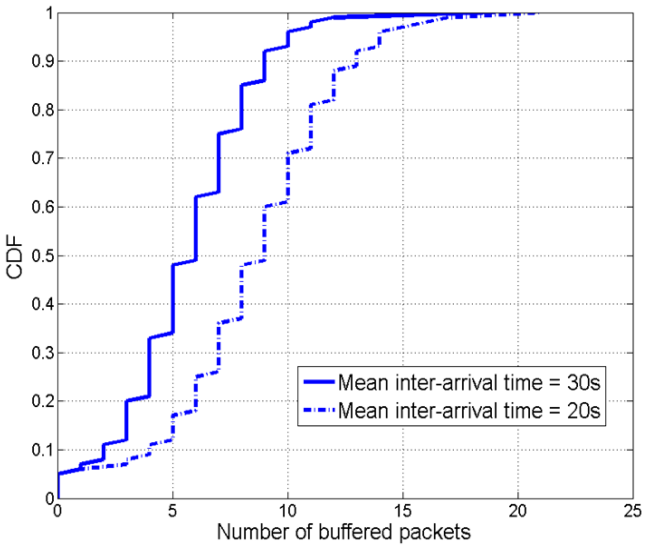

FIGURE 6. CDF of buffered packets.

All the curves almost coincide with each other because $T_{buffer} \gg T_{prom} + T_{rc} + T_{pg}$ and $T_{latency}$ is dominated by T_{buffer}, which is independent from the number of UEs

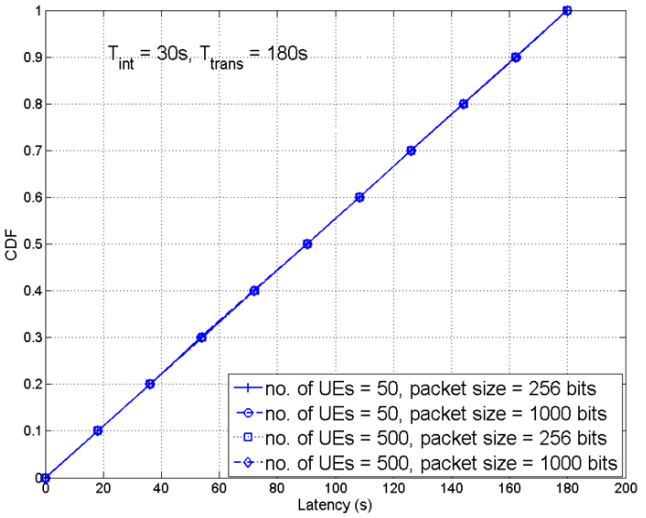

FIGURE 7. CDF of latency.

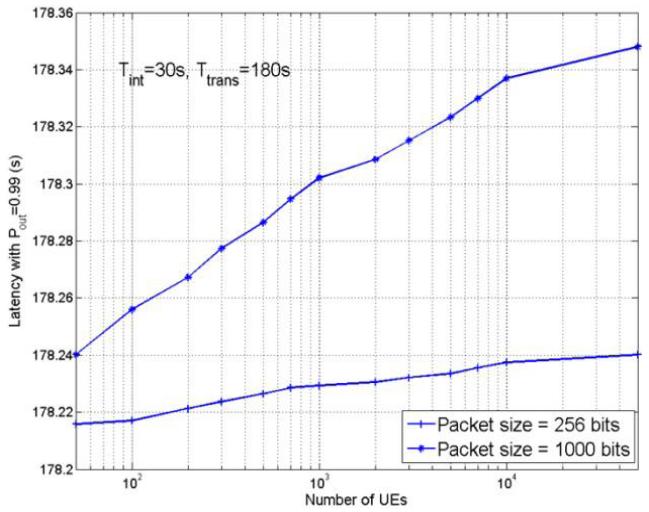

FIGURE 8. Latency ($P_{out} = 0.01$).

and the packet size. If we define the outage probability as $P_{out} = \Pr(T_{latency} \le \text{target } T_{latency})$, the latency values with $P_{out} = 0.01$ are depicted in Fig. 8.

We notice that latency increases with both the number of UEs and the packet size. However, given a larger packet size, latency is more sensitive to the number of UEs. Considering the fact that the packet size for MTC UEs is normally very small, latency will not be severely degraded even with a very large number of MTC UEs. When much smaller T_{int}, T_{trans} and a large packet size are considered, the duration of the transmission, i.e., T_{rc} becomes comparable with T_{buffer} and thus the curves are no longer overlapping as shown in Fig. 9. Moreover, the same trend is observed for latency with 0.01 outage probability in Fig. 10.

Table 4 compares the constraints and the actual results based on system level simulations. Clearly, all the constraints are satisfied.

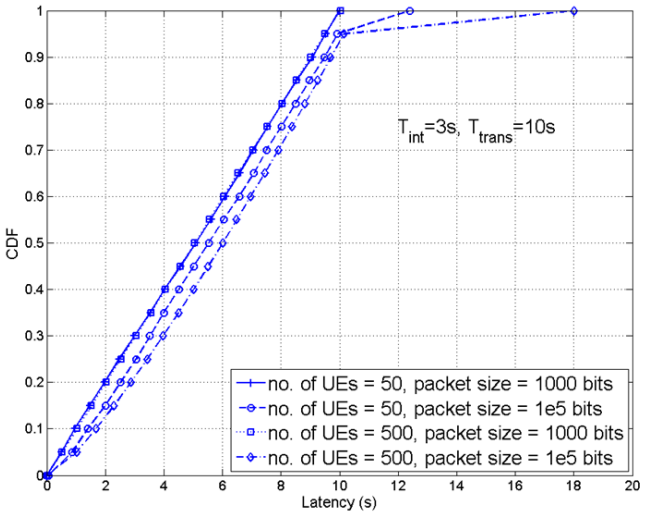

FIGURE 9. CDF of latency.

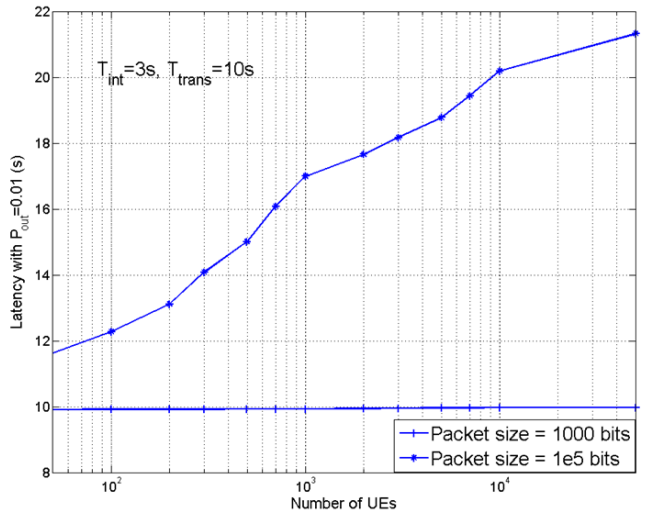

FIGURE 10. Latency (P_{out} = 0.01).

TABLE 4. Constraints vs. simulation results.

Parameters	Constraints	Actual Values
Maximal delay (s)	250	179.9914
Average delay (s)	150	90.2613
99% delay (s)	200	178.0906
$P_{fal} \leq 0.05$	0.05	0.0024
$P_K \geq 0.9$ (K=2)	0.9	0.9925

Next the energy efficiency analysis is conducted considering the DRX parameters and UE power model defined in [22] as listed in Table 5. Considering the small size of the MTC traffic packets, unlike in [22] where the target traffic is normal LTE traffic such as web surfing, here T_i and T_{tail} are chosen to be small values.

Fig. 11 depicts the CDF of average power of MTC users in terms of Watts for the proposed SPRST protocol and

TABLE 5. DRX parameters and UE power model.

Parameters	Value	Power (mW)
T_i	0.01	Depending on throughput
T_{is}	0.02	N/A
T_{on}	0.001	1680
T_{oni}	0.043	594
T_{ps}	0.02	1060
T_{pl}	0.04	1060
T_{pi}	1.28	11.4
T_{prom}	0.26	1210
T_{tail}	0.01	1060

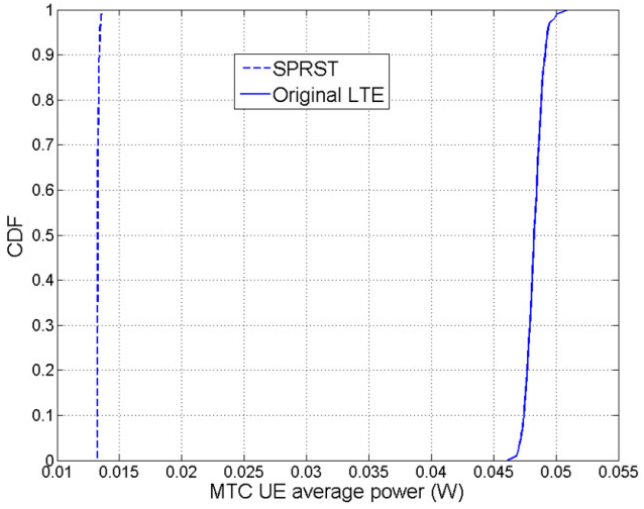

FIGURE 11. Energy consumption.

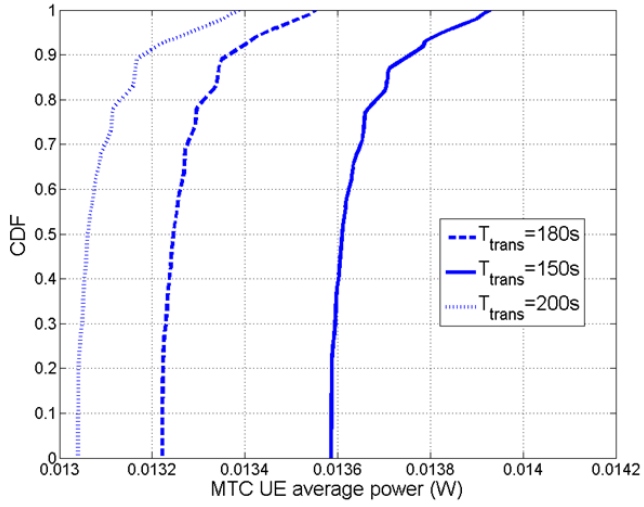

FIGURE 12. Energy consumption.

original LTE RRC protocol, where the RRC state transition is triggered by incoming traffic. It is clearly shown that the average energy consumption is reduced by around 90% due to the following reasons:

1) Less number of RRC state transitions, e.g., fewer promotions;

2) No paging in RRC_Idle for SPRST;
3) As mentioned above, the RRC inactivity timer is not needed and RRC connection is released once the eNB buffer is cleared and no uplink transmission is detected. Hence, UE stays in DRX mode in RRC_Connected state for a much shorter time and thus the energy consumption during DRX cycle in RRC_Connected state is saved.

Fig. 12 also compares the average MTC UE power for different T_{trans} values. It is illustrated that a shorter T_{trans} leads to a higher average power. This is mainly because a shorter T_{trans} means more RRC state transitions.

V. CONCLUSIONS

A novel RRC protocol is designed for MTC devices in LTE networks in this paper. Compared with DRX, which is basically a MAC layer operation targeting at the UEs with high traffic demand and medium to high mobility, the proposed scheme operates in the RRC layer. The existing schemes of discontinuous transmission and reception do not take traffic pattern into consideration thus are less adaptive to traffic variations. On the contrary, the proposed scheme takes advantage of the unique properties of MTC devices: long inter-arrival time, small packet size and extremely low mobility, and is more adaptive to the traffic pattern changes in the sense that the parameters are determined by the measurement results via exploiting the network memory, which has not been taken into consideration before. With the proposed new protocol, monitoring the paging occasions in RRC_Idle state is not needed and the RRC signalling overhead as well as energy consumption can be significantly reduced. It is proposed in 3GPP that M2M devices operate on a different narrow bandwidth from normal LTE UEs [8], [31]. By doing this, the MTC traffic and normal LTE traffic are separated and thus different RRC protocols can be easily employed simultaneously.

APPENDIX A

The DRX timers are listed and their meanings are explained in Table 6. The length of these timers is in general a trade-off between eNB scheduler freedom and UE power saving opportunity. Some examples are given in Fig. 13.

Whenever PDCCH indicates a new transmission for either downlink or uplink, the DRX on duration is extended by '*drx-InactivityTime*'. For downlink HARQ process, each subframe where the UE may expect a retransmission is a beginning of a number of subframes of on duration defined by '*drx-RetransmissionTimer*'. The DRX also goes into activity time whenever the UE sends a Scheduling Request (SR) in the Physical Uplink Control Channel (PUCCH).

There are two different ways for the UE to enter DRX opportunity: 1) the UE enters DRX opportunity once the DRX inactivity timer expires, and 2) the network sends a DRX command by setting the Logic Channel ID (LCID) in the MAC sub-header [15], [34]. Two different DRX cycles are defined as follows:

- Long DRX cycle: the fundamental cycle length that is always present in DRX.
- Short DRX cycle: optional, if short DRX is configured, the UE enters short DRX mode at the beginning of each DRX cycle, and enters long DRX mode after the DRX short cycle timer expires.

TABLE 6. DRX parameters [33].

Parameter	Description
DRX Cycle	The duration of 'On time' + 'OFF time'
onDurationTimer	The duration of 'On time' within one DRX cycle
drx-InactivityTimer	How long UE should remain 'ON' after the reception of a PDCCH.
drx-RetransmissionTimer	The maximum number of consecutive PDCCH subframes the UE should remain active to wait for an incoming retransmission.
shortDRX-Cycle	DRX cycle which can be implemented within the 'OFF' period of a long DRX cycle.
drxShortCycleTimer	Number of subframes the UE should follow the short DRX cycle.

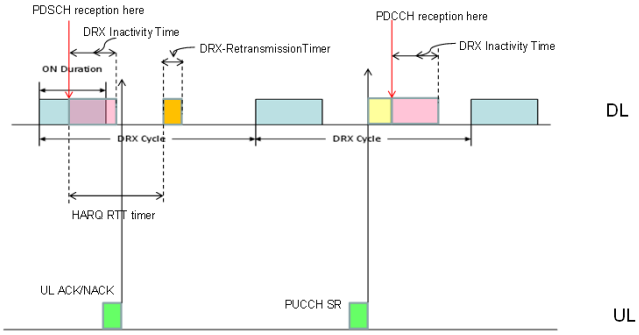

FIGURE 13. DRX operation in RRC_Connected state.

REFERENCES

[1] M. Zorzi, A. Gluhak, S. Lange, and A. Bassi, "From today's INTRAnet of Things to a future INTERnet of Things: A wireless- and mobility-related view," *IEEE Wireless Commun.*, vol. 17, no. 6, pp. 44–51, Dec. 2010.
[2] T. Taleb, A. Ksentini, and A. Kobbane, "Lightweight mobile core networks for machine type communications," *IEEE Access*, vol. 2, pp. 1128–1137, Sep. 2014.
[3] M. Condoluci, M. Dohler, G. Araniti, A. Molinaro, and K. Zheng, "Toward 5G DenseNets: Architectural advances for effective machine-type communications over femtocells," *IEEE Commun. Mag.*, vol. 53, pp. 134–141, Jan. 2015.
[4] D. Triantafyllopoulou *et al.*, "D3.5: Energy efficient discover mechanisms of candidate networks and neighbour nodes," C2POWER, U.K., Tech. Rep. D3.5, Jan. 2013. [Online]. Available: http://www.ict-c2power.eu/images/Deliverables/C2POWER_D3.5.pdf
[5] A. Lioumpas *et al.*, "D2.4: The EXALTED system concept and its performance," EXALTED, Greece, Tech. Rep. D2.4, Feb. 2013. [Online]. Available: http://www.ict-exalted.eu/fileadmin/documents/EXALTED_WP2_D2.4-final.pdf
[6] P. Jain *et al.*, "System improvements for machine-type communications (MTC)," 3GPP, Valbonne, France, Tech. Rep. 23.888, Sep. 2012.
[7] "Service requirements for machine-type communications (MTC); stage 1," 3GPP, Valbonne, France, Tech. Rep. 22.368, Dec. 2014.
[8] P. Bhat *et al.*, "Study on provision of low-cost MTC UEs based on LTE," 3GPP, Valbonne, France, Tech. Rep. 36.888, Jun. 2012.

[9] "Machine-type and other mobile data applications communications enhancements," 3GPP, Tech. Rep. 23.887, Jul. 2013.
[10] D. Flore. (Feb. 18, 2015). *Evolution of LTE in Release 13*. [Online]. Available: http://www.3gpp.org/news-events/3gpp-news/1628-rel13
[11] R. Fedrizzi and T. Rasheed, "Cooperative short range routing for energy savings in multi-interface wireless networks," in *Proc. VTC*, Dresden, Germany, Jun. 2013, pp. 1–5.
[12] A. P. Miettinen and J. K. Nurminen, "Energy efficiency of mobile clients in cloud computing," in *Proc. HotCloud*, Berkeley, CA, USA, 2010, pp. 4–10.
[13] L. Zhang and D. Qi, "Energy-efficient task scheduling algorithm for mobile terminal," in *Proc. IET Int. Conf. Wireless, Mobile Multimedia Netw.*, Hangzhou, China, Nov. 2006, pp. 1–4.
[14] X. Ma, Y. Cui, L. Wang, and I. Stojmenovic, "Energy optimizations for mobile terminals via computation offloading," in *Proc. PDGC*, Solan, India, Dec. 2012, pp. 236–241.
[15] "Details of MAC DRX control," 3GPP TSG-RAN WG2, Tech. Rep. R2-080934, Feb. 2008.
[16] P. Sudarsan *et al.*, "Information model for type 1 interface HeNB to HeNB management system (HeMS)," 3GPP, Valbonne, France, Tech. Rep. 32.592, Dec. 2014.
[17] A. T. Koc, S. C. Jha, R. Vannithamby, and M. Torlak, "Optimizing DRX configuration to improve battery power saving and latency of active mobile applications over LTE-A network," in *Proc. WCNC*, Apr. 2013, pp. 568–573.
[18] S. Fowler, R. S. Bhamber, and A. Mellouk, "Analysis of adjustable and fixed DRX mechanism for power saving in LTE/LTE-advanced," in *Proc. IEEE ICC*, Ottawa, ON, Canada, Jun. 2012, pp. 1964–1969.
[19] H.-C. Wang, C.-C. Tseng, G.-Y. Chen, F.-C. Kuo, and K.-C. Ting, "Power saving by LTE DRX mechanism using a mixture of short and long cycles," in *Proc. IEEE TENCON*, Xi'an, China, Oct. 2013, pp. 1–6.
[20] S. C. Jha, A. T. Koc, R. Vannithamby, and M. Torlak, "Adaptive DRX configuration to optimize device power saving and latency of mobile applications over LTE advanced network," in *Proc. IEEE ICC*, Budapest, Hungary, Jun. 2013, pp. 6210–6214.
[21] A. T. Koc, S. C. Jha, R. Vannithamby, and M. Torlak, "Device power saving and latency optimization in LTE-A networks through DRX configuration," *IEEE Trans. Wireless Commun.*, vol. 13, no. 5, pp. 2614–2625, May 2014.
[22] J. Huang, F. Qian, A. Gerber, Z. M. Mao, S. Sen, and O. Spatscheck, "A close examination of performance and power characteristics of 4G LTE networks," in *Proc. MobiSys*, Low Wood Bay, U.K., Jun. 2012, pp. 225–238.
[23] AT&T. *Comparing LTE and 3G Energy Consumption*. [Online]. Available: http://developer.att.com/application-resource-optimizer/docs/best-practices/comparing-lte-and-3g-energy-consumption, accessed May 2, 2015.
[24] S. Deng and H. Balakrishnan, "Traffic-aware techniques to reduce 3G/LTE wireless energy consumption," in *Proc. ACM CoNEXT*, Nice, France, Dec. 2012, pp. 181–192.
[25] *Evolved Universal Terrestrial Radio Access (E-UTRA); Radio Resource Control (RRC)*, 3GPP Standard TS 36.331, Mar. 2015.
[26] W. Kai and L. Lihua, "Research and implementation of LTE RRC connection establishment process of network side," in *Proc. ICEIT*, Chongqing, China, Sep. 2010, pp. 229–232.
[27] S. Zhang, Z. Zhao, H. Guan, D. Miao, and H. Yang, "Statistics of RRC state transition caused by the background traffic in LTE networks," in *Proc. IEEE WCNC*, Shanghai, China, Apr. 2013, pp. 912–916.
[28] Z. Huawei, C. Ping, H. Lin, and L. Fuchang, "The enhance mechanism of RRC connection release in LTE system," in *Proc. Int. Conf. IETICT*, Beijing, China, Apr. 2014, pp. 459–464.
[29] *3GPP Work Programme*. [Online]. Available: http://www.3gpp.org/DynaReport/GanttChart-Level-2.htm#bm570030, accessed May 2, 2015.
[30] *MIT Online Course*. [Online]. Available: http://ocw.mit.edu/courses/electrical-engineering-and-computer-science/6-262-discrete-stochastic-processes-spring-2011/course-notes/MIT6_262S11_chap02.pdf, accessed May 2, 2015.
[31] *Coverage Extension for MTC UEs*, document R1-125204, Nov. 2012.
[32] H. Holtkamp *et al.*, "D2.2: Definition and parameterization of reference systems and scenarios," EARTH, Germany, Tech. Rep. D2.2, Jun. 2010. [Online]. Available: https://www.ict-earth.eu/publications/deliverables/deliverables.html
[33] *ShareTechNote*. [Online]. Available: http://www.sharetechnote.com/html/MAC_LTE.html, accessed May 2, 2015.
[34] S. Kangude. *Lecture: LTE Scheduling and DRX*. [Online]. Available: http://lyle,smu.edu/~skangude/eets8316.html, accessed May 2, 2015.

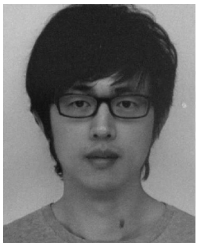

YINAN QI received the B.Sc. degree in electronics and information theory and the M.Sc. degree in mobile communications from Peking University, Beijing, China, in 2000 and 2003, respectively, and the Ph.D. degree in electronics engineering from the University of Surrey, Surrey, U.K. He is currently a Research Fellow with the Institute for Communication Systems, University of Surrey. His main research interests include cooperative communications; coding, analysis, and systematic modeling of future cellular systems; and green communications.

ATTA UL QUDDUS received the M.Sc. degree in satellite communications and the Ph.D. degree in mobile cellular communications from the University of Surrey, U.K., in 2000 and 2005, respectively. He is currently a Lecturer in Wireless Communications with the Institute of Communications, Department of Electronic Engineering, University of Surrey. During his research career, he has led several national and international research projects that contributed toward 3GPP standardization. His current research interests include machine type communication, cloud radio access networks, and device-to-device communication. In 2004, he received the Centre for Communications Systems Research Excellence Prize sponsored by Vodafone for his research on adaptive filtering algorithms.

MUHAMMAD ALI IMRAN (SM'12) received the M.Sc. (Hons.) and Ph.D. degrees from Imperial College London, U.K., in 2002 and 2007, respectively. He has led a number of multimillion international research projects encompassing the areas of energy efficiency, fundamental performance limits, sensor networks, and self-organizing cellular networks. He has a global collaborative research network spanning both academia and key industrial players in the field of wireless communications. He has supervised 20 successful Ph.D. graduates, and authored over 200 peer-reviewed research papers, including over 20 IEEE TRANSACTIONS papers. He is currently a Reader (an Associate Professor) with the Institute for Communication Systems, University of Surrey, U.K. He leads the new physical layer work area with the 5G Innovation Centre and the curriculum design for the Engineering for Health program in Surrey. He is a Senior Fellow of the Higher Education Academy, U.K. He was a recipient of the IEEE Comsoc's Fred Ellersick Award in 2014, the FEPS Learning and Teaching Award in 2014, and he was twice nominated for the Tony Jean's Inspirational Teaching Award. He was a Shortlisted Finalist of the Wharton-QS Stars Awards for his innovative teaching and VC's learning in 2014, and received the teaching award from the University of Surrey. He has delivered several keynotes, plenary talks, invited lectures, and tutorials in many international conferences and seminars. He has been a Guest Editor of the Special Issues of the *IEEE Communications Magazine*, the *IEEE Wireless Communication Magazine*, *IET Communications*, and the IEEE ACCESS. He is an Associate Editor of the IEEE COMMUNICATIONS LETTERS and the *IET Communications* journal.

RAHIM TAFAZOLLI (SM'09) is currently a Professor and the Director of the Institute for Communication Systems and the 5G Innovation Centre with the University of Surrey, U.K. He has authored over 500 research papers in refereed journals and international conferences, edited two volumes of books entitled *Technologies for Wireless Future* (Wiley, Vol.1 2004 and Vol.2 2006), and has been an Invited Speaker. He was appointed as a fellow of the Wireless World Research Forum in 2011, in recognition of his personal contribution to the wireless world, and is heading one of Europe's leading research groups.